PCCP

View Online
Dynamic Article Links

Cite this: *Phys. Chem. Chem. Phys.*, 2011, **13**, 16366–16372

www.rsc.org/pccp

PAPER

Fluorescence enhancement at hot-spots: the case of Ag nanoparticle aggregates†

Ron Gill‡*[a] and Eric C. Le Ru[b]

Received 1st April 2011, Accepted 24th July 2011
DOI: 10.1039/c1cp21008d

We report the enhancement of the fluorescence emitted from dye-labeled DNA upon co-aggregation with silver nanoparticles. The co-aggregation process is induced by the polycationic molecule spermine, which both neutralizes the charge of the DNA backbone and aggregates the nanoparticles. This simple method generates nanoparticle aggregates with very short (1–2 nm) inter-particle distance. Even though no spacer layer was used, large enhancements of the fluorescence, in the range of 15–740× (depending on the original quantum yield of the dye used), were observed. Theoretical modeling shows that this occurs as the local enhancement of the electromagnetic field near the hotspots is sufficiently large to overcome the quenching by the surface, even at short distances of 1 nm. The predicted trend of increased SEF enhancement with a decrease in initial quantum yield is observed. The average enhancements observed in this system are on-par with the best results obtained on nanostructured surfaces to date.

Introduction

It is well known that noble metal nanoparticles exhibit optical properties that are markedly different from the properties of the bulk metals. For instance, light can couple to coherent oscillations of conduction electrons (known as a Localized Surface Plasmon, LSP) on the surface of the nanoparticles.[1] Depending on composition, shape and size, a specific resonant frequency exists at which the interaction of light with these localized surface plasmons is maximal. When excited near this resonance frequency, very strong electromagnetic fields are created near the surface of the nanoparticles. These strong fields can enhance the interaction of light with molecules in the vicinity of the surface,[2–5] giving rise to phenomena such as surface-enhanced Raman scattering (SERS) and surface-enhanced fluorescence (SEF). It has long been known, both from theoretical and experimental studies, that the enhanced fields in between nanoparticles (known as "hot spots") are much stronger than those around single nanoparticles and thus much larger enhancements are expected.[2,6,7]

To date, much of the research effort in surface-enhanced spectroscopy is directed toward SERS, where average enhancement factors (EFs) of 10^5–10^6 (maximum EFs of 10^8–10^{10}) are typically observed both on nano-structured substrates and on nanoparticle aggregates in solution.[8] However, to date very limited research was done in the field of SEF, although SEF was experimentally detected[9] and subsequently theoretically explained[10] only a few years after SERS. Additionally, unlike SERS, most of the published research in SEF is done on nano-structured surfaces[11–13] or on single nanoparticles,[14–18] and very few reports exist on efficient SEF in nanoparticle aggregate systems.[19–22] This may arise from the fact that most research on SEF from nano-structured surfaces and single nanoparticles, has shown that the fluorophore must be at least 5–10 nm from the metal surface for the surface enhancement to overcome the quenching from the surface.[23–26] However, theoretical predictions of the enhancements in hot-spots between nanoparticles show that the electromagnetic fields are so strong, that efficient SEF could occur *even when the fluorophore is just 1–2 nm* from the surface.[27,28] Thus, it would seem rather surprising, that although researchers in the field of SERS have been aggregating silver or gold nanoparticles together with dyes for three decades, evidence of high fluorescence enhancement for molecules adsorbed as close as 1–2 nm from the surface has not been reported so far.

[a] *Philips Research, High Tech Campus, 5656 AE Eindhoven, The Netherlands*
[b] *The MacDiarmid Institute for Advanced Materials and Nanotechnology, School of Chemical and Physical Sciences, Victoria University of Wellington, P.O. Box 600, Wellington 6140, New Zealand*

† Electronic supplementary information (ESI) available: Mrad and Mtot for a nanoparticle dimer as a function of position, at resonance and off resonance; Calculation of the SERRS enhancement factor for R6G-labeled DNA; Overlap of dye spectra with Plasmon resonance peak of the Ag NP; Calculation of the quantum yield of the different dyes attached to DNA; Surface coverage of the DNA on the Ag NPs and effect of DNA concentration on SEF enhancement; Graphs of fluorescence enhancement for HEX and R6G-labeled DNA2; Control experiments; TEM images of aggregated Ag-NPs. Theoretical calculations of the effect of increased distance from the surface on the reduction of the observable (average) SERS signal. Reproducibility of the SEF signals. See DOI: 10.1039/c1cp21008d

‡ Current Address: MIRA institute of biomedical technology and technical medicine, Faculty of Science and Technology, University of Twente, P.O. Box 217, 7500 AE Enschede, The Netherlands. Fax: + 31 53 4891105; Tel: + 31 53 4893161; E-mail: r.gill@utwente.nl.

Here we present theoretical predictions of the average SEF signal for a simple model system: a dimer of closely spaced metallic spheres. They indicate that the observed quenching for dye randomly adsorbed in an aggregated nanoparticle system can be explained by a combination of the random distribution of dye positions and the imperfection in physical and spectral alignment in real-life experiments. However, for dyes that are not adsorbed on the surface, but are still very close (1 nm) the theoretical model predicts that enhancement should be possible. We then show experimentally that in a system where dye-labeled DNA is used to get the dye close to the surface, but not adsorbed on it, efficient SEF, with average enhancement factors in the range of 15–750× (depending on fluorophore quantum yield), is observed.

Theoretical background

In order to understand the key factors affecting the fluorescence enhancement or quenching in silver nanoparticle aggregates, while looking at effects of position distribution, distance from surface *etc*., we carried out electromagnetic calculations of the field enhancements in one of the simplest model structure containing an EM hot-spot: a dimer formed by two identical closely-spaced spheres. Although an over-simplification of the real nanoparticle aggregates, the dimer model captures, at least semi-quantitatively, the key features of substrates with EM hot-spots.[6–8,29,30] Moreover, the theoretical tools required for such a calculations are well established.[31,32] We therefore here only recall the most important aspects of such a calculation (with further details provided in the supplementary information†) and discuss their implications for our SEF experiments.

We use geometrical parameters that correspond to the best estimates for our experiments: Ag sphere radius of 17 nm, gap between spheres of 2 nm, and embedding medium is water (see supporting information for TEM images of the particle aggregates†). Calculations were carried out using generalized Mie theory as in ref. 30 and its generalization to the case of excitation by a dipolar emitter.[33,34] For clarity, we here briefly recall without justification the main results from the EM theory of SERS and SEF. Using the notations of ref. 2, the predicted SERS EF at a given point in space (in the $|E|^4$ approximation for zero-Raman-shift[35]) is given by:

$$M_{\mathrm{SERS}} = [M_{\mathrm{Loc}}(\lambda_{\mathrm{L}})]^2 \qquad (1)$$

Where $M_{\mathrm{Loc}}(\lambda_{\mathrm{L}}) = |E|^2/|E_0|^2$ is the standard local field intensity enhancement at the excitation wavelength λ_{L}. SEF profits, like SERS, from the enhancement factor $M_{\mathrm{Loc}}(\lambda_{\mathrm{L}})$ for excitation from the ground state to the excited state. The situation in emission is more complicated (see ref. 2, 6, 27 for full details) and does not result in any enhancement for a fluorophore with a good quantum yield. To calculate its contribution, we must take into account both the modification of the radiative emission (following the same EF as the emission part of the SERS EF) and the additional possibility of non-radiative emission into the metal. Overall, this results in an expression for the SEF EF that has similarities with that of the SERS EF. Explicitly, ignoring spectral profile modifications,[27] the SEF EF in the $|E|^4$ approximation for zero-Stokes-shift is given by:[2,27]

$$M_{\mathrm{SEF}} = [M_{\mathrm{Loc}}(\lambda_{\mathrm{L}})]^2/(QM_{\mathrm{Tot}}) \qquad (2)$$

where M_{Tot} is the total (radiative + non-radiative) decay rate EM enhancement and is assumed to dominate non-radiative decay (*i.e*. is larger than $(Q_0)^{-1}$, Q_0 being the non-modified quantum yield of the fluorophore). Note that this expression predicts a simple scaling of the SEF EF with $(Q_0)^{-1}$. We will therefore only consider the case $Q_0 = 1$ in the theoretical section. M_{Tot} can be calculated within standard classical EM theory as explained for example in a general context in ref. 2, 31, 32. For the relevant case here of sphere dimers, we have used the methods described in ref. 33, 34 to calculate it.

Examining first the predicted enhancements for the best possible situation – a fluorophore in the exact center of a dimer with incident polarization along the dimer axis, we see that enhancements of up to 10^3–10^4 are possible despite the close proximity to the metallic surface and even for fluorophores with a quantum yield of unity, Fig. 1. However, in practice, the fluorophores are randomly distributed and are only rarely situated at the point of highest enhancement. Therefore, we calculated M_{Loc} and M_{Tot} *as a function of position on the surface* for four distances (d = 0.2, 0.5, 1 and 1.5 nm) and two model cases: Firstly at resonance (of the dimer LSP) where the field enhancements are large (λ_{L} = 497 nm and polarization along dimer axis) and secondly off resonance (λ = 562 nm) in a situation where these enhancements are much more moderate (see supporting information for results and discussion of these calculations†). The fluorescence EFs, M_{SEF}, were deduced using eqn (2), and their spatial distributions on the surface are shown in Fig. 2(a) and (b), along with the average fluorescence EF $< M_{\mathrm{SEF}} >$ for each case (this is the surface average for a random distribution of molecules on the dimer).

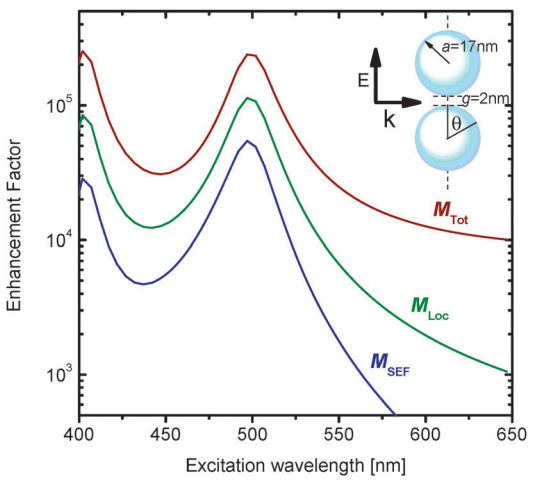

Fig. 1 Wavelength dependence of the enhancement factors predicted for a fluorophore at the centre of the gap (gap size = 2 nm) of a silver dimer (NP radius = 17 nm) embedded in water (see schematic, top right): M_{Loc} is the local field intensity EF, M_{Tot} the total EM decay rate EF, and M_{SEF} the approximate fluorescence EF (eqn (2)). Excitation polarization and fluorescence dipole are both taken aligned along the dimer axis.

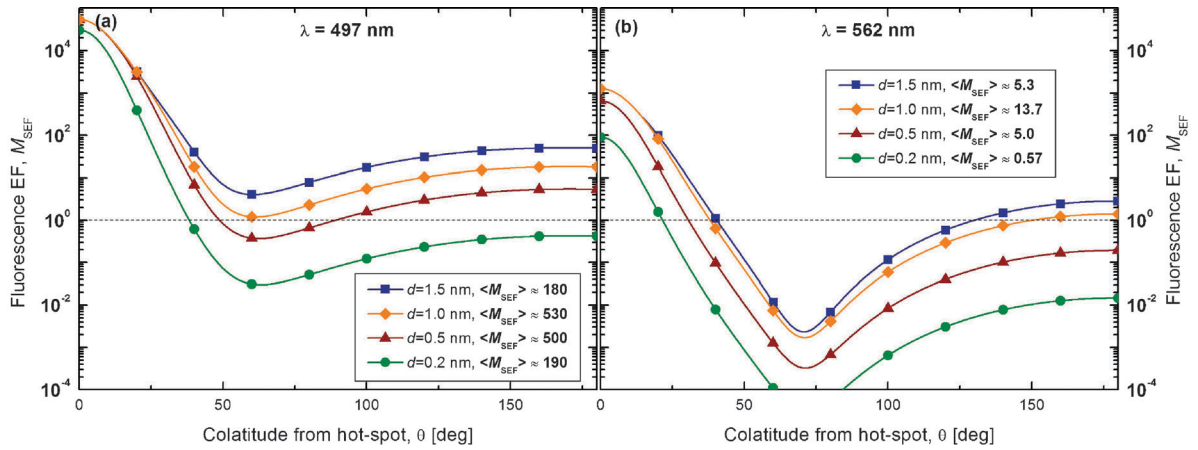

Fig. 2 Distribution of the enhancement factor M_{SEF} (for the same dimer model as in Fig. 1) as a function of fluorophore position on the dimer surface, characterized by the colatitute (angle θ) from the hot-spot (*i.e.* θ = 0 in the gap). (a) excitation at resonance, (b) excitation 65 nm redshifted from resonance peak. Four distances, *d*, from the surface are considered. In the case of *d* = 1.5 nm, the distribution is cut-off below θ = 13 degrees because the fluorophores cannot fit in the gap while maintaining the same distance from the surface. The surface-averaged fluorescence EFs corresponding to these distributions are also given in (a) and (b).

In Fig. 2(a) we see that at resonance, there is a very high enhancement of the fluorescence at the hotspot, which is almost independent of the distance at which the fluorophore is positioned. This gives high average SEF EF in the order of a few hundred at all 4 distances.

However, in practice, there are several other factors (except for random position distribution) which all tend to reduce the final observable SEF EF. These factors – random orientation of the dimer axis compared to excitation polarization, random orientation of the molecular dipole axis compared to the dimer axis, and off resonance position (of at least one) of the excitation and emission wavelengths – all cause a large reduction in the excitation enhancement and decay rate enhancement, with only a small effect on the non-radiative decay rate.

Therefore we qualitatively explore these effects by looking at only one factor – off resonance excitation of the Plasmon (see supplementary information for a detailed discussion†).

Fig. 2(b) shows that in such a case, even though for dye adsorbed to the surface, (who will behave more closely to the case of d = 0.2 nm), quenching might be observed, under similar conditions enhancement could be observed if the distance of the dye from the surface can be increased to 1–1.5 nm. (Because of the nature of the logarithmic scale used in Fig. 2(b), the area below the M = 1 line apprears larger then that above it, and yet the average enhancement is greater than one for all distances except for the d = 0.2 nm) In the following, we therefore focus on providing an experimental demonstration of this effect in silver nanoparticle aggregates, using dye-labelled DNA as a means to control the distance between the fluorophore and the nanoparticle surface.

Experimental section

Reagents

DNA-1 used for comparison of different nanoparticles had the following sequence:

5′-R6G-tcatttcacgcaaactgttggccactatgagttaaactt – 3′.

DNA-2 had the sequence:

5′-dye-tggaagttagattgggatcatagcgtcat-3′.

These custom-made dye-labeled oligonucleotides were custom synthesized by IBA GmbH (Göttingen, Germany). All other chemicals were purchased from Sigma-Aldrich.

Nanoparticle synthesis

Citrate-coated Ag nanoparticles were synthesized according to a modified Lee and Meissel procedure.[36] In brief, silver nitrate (90 mg) was dissolved in distilled water (500 ml) and heated to near boiling under stirring. A sodium citrate solution was added (10 ml, 1%) and the solution held at boiling for 90 min with continuous stirring.

Hydroxylamine-coated Ag nanoparticles were synthesized according to a modified Leopold and Lendl procedure.[37] In brief, 1 ml of a hydroxylamine hydrochloride/sodium hydroxide solution (15 mM/30 mM, respectively) was added to 9 ml of a less concentrated silver nitrate solution (1.11 mM) under rapid stirring.

EDTA-coated Ag nanoparticles were synthesized according to a modified literature procedure.[38] In brief, 500 ml of a 0.16 mM EDTA solution containing 4 mM NaOH was heated to boiling under stirring. 5 ml of 0.26 mM $AgNO_3$ solution was added in 4 aliquots of 1.25 ml, and the solution was held at boiling for 20 min with continuous stirring.

Measurement of fluorescence

Fluorescence was measured on a Raman Systems R-3000 Raman spectrometer with a 532 nm laser excitation. The power setting used corresponds to 11 mW at the probe focal point (focal spot diameter is 100 μm). The spectrometer was calibrated using a white light lamp with a 3300 K black body profile.

SERRS/SEF measurements

For initial SERRS/SEF measurement, as synthesized Ag-nanoparticles were diluted in 10 mM Tris buffer, pH = 7.4, containing 0.01% Tween (TT buffer) to a concentration equivalent to 2 O.D.

(which is about 160 pM). For SEF measurements in optimized conditions, as synthesized Ag-nanoparticles were diluted in 10 mM Phosphate buffer, pH = 7.1, to a concentration equivalent to 2 O.D. In both cases, 20 μL of Dye-DNA diluted in water was mixed with 20 μL of 100 μM spermine in TT buffer, and then 60 μL of the diluted Ag nanoparticles were added. Final concentration of dye-labeled DNA was 500 pM. The Raman/fluorescence spectra were measured 20 s after the addition of the nanoparticles.

Dynamic light scattering (DLS) measurements

Dynamic light scattering (DLS) measurements done after 20 s of aggregation show that the average hydrodynamic size of the clusters in the solution is only 1.5× larger than that of single particles. This suggests that most colloidal clusters are between dimers and tetramers, rather than larger aggregates. DLS measurements were done on a Dynapro Titan (Wyatt Technology, USA).

Experimental results and discussion

To develop a system in which the properties of a wide variety of fluorophores can be tested, we have used dye-labeled DNA and a polyamine-based aggregation of silver nanoparticles as described previously.[39] This bottom-up approach of chemical aggregation produces aggregates with nanoparticle spacing of the order of 1–2 nm. By comparison, the smallest spacing achieved consistently by top-down approaches, such as e-beam nanolithography, is currently of the order of 10 nm. Moreover, by using the interaction of the DNA and the polyamine to bring the fluorophore close to the silver surface and not the specific chemistry of the fluorophore, it is possible to use fluorophores that do not adsorb spontaneously to silver. This approach is depicted in Fig. 3. We use a 532 nm laser excitation, and dyes that are efficiently excited at this wavelength, as the plasmon peak of the silver nanoparticle aggregates is very close to this wavelength (See Supporting Information).

From the theoretical predictions presented above we concluded that a possible explanation for the lack of significant SEF in SERS experiments that involved co-aggregation of dyes and silver nanoparticles is that the dye molecules typically adsorb directly on (or are positioned very close to) the nanoparticle surface, thus giving an average quenching signal for short fluorophore to surface distances, as predicted in Fig. 2(b). To test this assumption, we measured the fluorescence enhancement under the conditions that are usually used in the literature to get efficient SERS with silver nanoparticle aggregates. When examining the uncorrected spectrum emitted from aggregation of citrate-reduced silver nanoparticles with dye-labeled DNA, one can see a combined signal of fluorescence and Raman scattering, Fig. 4 (black curve). While the measured surface enhanced resonant Raman scattering (SERRS) average enhancements are rather high, of the order of 2×10^5 (see Supporting Information), the SEF enhancement is only ~2 (when salt is added to further enhance the aggregation the SEF "enhancement" goes below 1). This results shows that although we used a DNA 'tail' to bind the dye to the silver surface, under the commonly used conditions, the dye would be very close to the surface producing large SERS enhancements and very small SEF enhancements.

With such an interpretation in mind, we have examined different nanoparticle capping agents to study whether nanoparticles with different organic capping agents produce different SEF enhancements. We have compared the signals from the Citrate-reduced silver nanoparticles[36] to those of two other common synthesis procedures-EDTA[38] (Ethylene diamine tetra-acetate) and hydroxylamine[37]-capped Ag nanoparticles. These methods were chosen as they all give about the same size of silver nanoparticles (30–40 nm diameter). As can be seen in Fig. 4, a small enhancement of the fluorescence is observed in addition to the enhanced Raman peaks for citrate and hydroxylamine-capped nanoparticles. However, for the EDTA coated nanoparticles (red curve) a reduced SERRS intensity and an increased fluorescence peak compared to the other types of nanoparticles is observed. This can be explained by the fact that EDTA is a much bulkier molecule, providing the EDTA-coated nanoparticles with the thickest organic shell of the three, thereby keeping the dye at a larger distance from the surface. Therefore, all further investigations were done on EDTA silver particles.

Changing the buffer in which the nanoparticles were diluted from Tris-Tween to Phosphate buffer, we found that the fluorescence signal was further enhanced, while the SERRS signal was further reduced (up to a level where it could hardly be seen above the fluorescent background), as shown in Fig. 5(a).

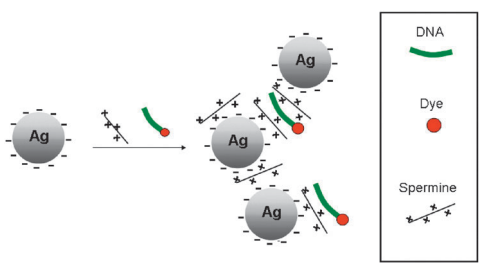

Fig. 3 Spermine induced co-aggregation of dye-labeled DNA and Ag nanoparticles.

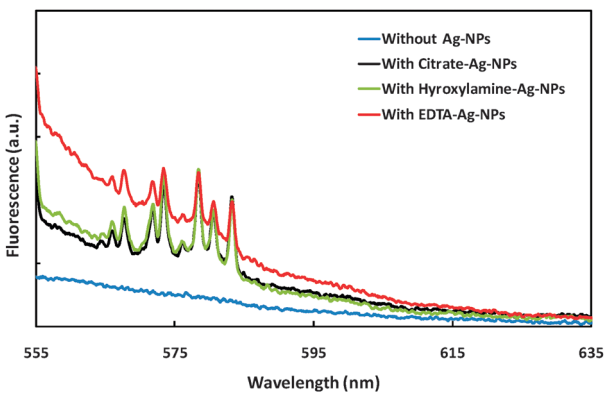

Fig. 4 Measured spectra of 500 pM R6G-labeled DNA-1, in absence (blue curve) and in the presence of citrate (black curve), hydroxylamine (green curve) or EDTA-coated (red curve) silver nanoparticles. All experiments were conducted in a solution containing 20 μM Spermine, and 4 mM Tris Buffer pH = 7.4 containing 0.01% Tween 20. The NPs concentration when they were present was 100 pM.

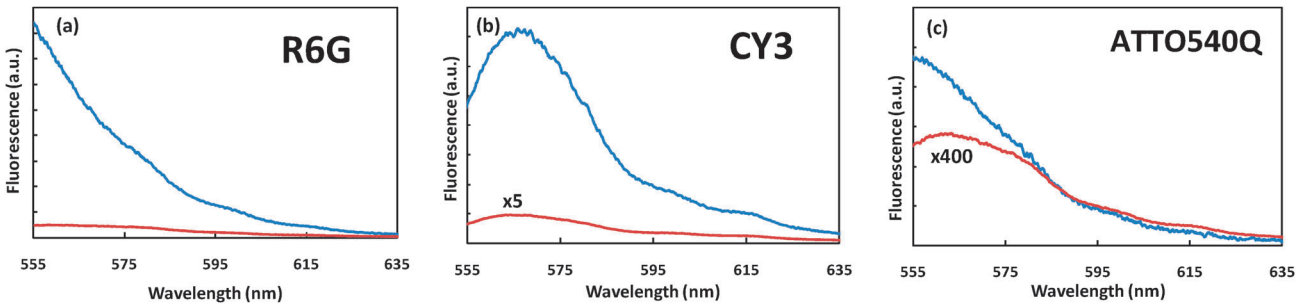

Fig. 5 Fluorescence spectra of 500 pM dye-labeled DNA, in the presence (blue line) and absence (red line) of EDTA-coated silver nanoparticles (Ag-NPs). (a) of R6G-labeled DNA-1 (b) of Cy3-labeled DNA-2 (c) of Atto540Q-labeled DNA-2. All experiments were conducted in a solution containing 20 μM Spermine, and 4 mM phosphate buffer pH = 7.1. The NPs concentration was 100 pM.

With the Phosphate buffer, the average SEF enhancement factor is about 17× for R6G-labeled DNA, while the average SERS EF is at least 10 times lower than with the Tris-Tween buffer. Both of these observations suggest that the distance of the fluorophores from the surface has increased.

In our first experiments we used R6G as a dye since it is well characterized for SERRS and it has a known resonant Raman cross section. Therefore it is the natural choice when comparing SERRS and SEF. As we are interested in the applications of SEF in the fields of biosensing and molecular diagnostics, we have also investigated dyes from other commonly used dye families such as fluorescein and cyanine derivatives. The most common dye used for DNA labeling that is excitable by a green laser (λ = 532 nm) is the cyanine-based dye Cy3. We have measured the QY of the Cy3-labeled DNA to be about half of the value we measured for the R6G labeled DNA (QY = 0.08 for Cy3 compared with 0.17 for R6G). As was shown in eqn (2), the enhancements should in a first approximation increase as the bare QY of the fluorophore, Q_0, decreases (when all other conditions remain identical).

In our experiments, as the silver nanoparticles are the same and the aggregation process is the same, one can therefore expect to measure higher enhancements with the lower quantum yield dyes such as Cy3, and this is indeed the case. Going from R6G-labeled DNA to Cy3, the enhancement increased to 37×, as expected, see Fig. 5(b). The enhancement value presented here are comparable to those published for nanostructures surfaces[40–45] when using dyes with similar quantum yields. Moreover, the enhancement factor did not change significantly when the dye concentration was 10× lower, as we expected for sub-monolayer concentrations of DNA (see supporting information†). For completeness, we have also studied DNA labeled with HEX (a fluorescein derivative) and the enhancement of R6G-labeled DNA of a different composition than the previous one (see supporing information for full details†). It is important to note, that for all dyes tested, the addition of spermine alone, without silver nanoparticles, or in the presence of silver nanoparticles without the aggregating agents, no significant change in fluorescence was observed. (see supporting information†). Plotting the enhancement factor *vs.* the quantum yield, Fig. 6, we see the expected trend, of increase in fluorescence enhancement with decrease of the initial quantum yield.

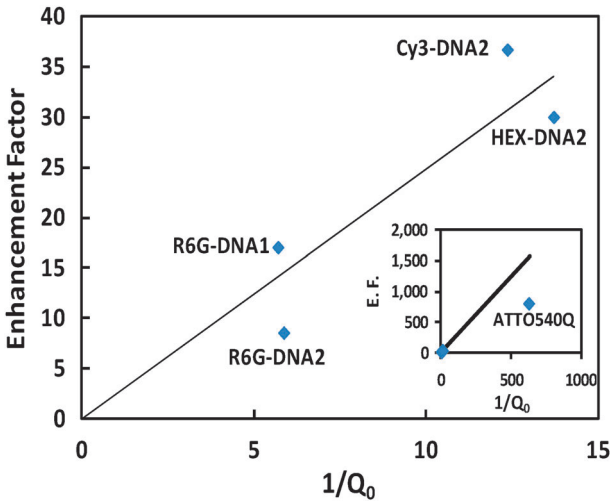

Fig. 6 SEF Enhancement factor *vs.* inverse of quantum yield plot for several dye-labeled DNA. Insert – extrapolation of the trendline from main figure toward the point of the quencher, Atto540Q. Error bars were omitted due to clarity but were all smaller or equal to the marker size (see supporting information for further details on the reproducibility of the measurements†).

The scatter of the results around the trendline originates from the effect of the DNA composition, and the way the exact chemistry of the dye influences the distance and orientation of the fluorophore from the nanoparticles. The three different dyes we used, have not only different chemical structures, but they also differ in charge (R6G is neutral, Cy3 is positively charged, and HEX is negatively charged). We plan to further investigate these effects in the future.

To continue along this line of reduced QY and enhanced SEF efficiency we also studied the SEF of a very low quantum yield dye, Atto 540Q. This rhodamine based dye is commonly used as a quencher in DNA based assays, and we determined a QY of $Q_0 = 1.6 \times 10^{-3}$ for Atto 540Q-labeled DNA. As shown in Fig. 5(c), we here observed an average SEF enhancement factor of 740×, one of the highest reported for average SEF measurements.[46] Comparing the average trend of enhancement factor *vs.* inverse of quantum yield, we can see (Fig. 6, insert) that the point for Atto540Q lies below the trendline. This may indicate that for this dye with a very low quantum yield, the assumption that the total non-radiative

rate is dominated by the non-radiative emission into the metal begins to fail in the present conditions.

Comparing our experimental results with the theoretical predictions, we see that although we used an oversimplified model, our results confirm the qualitative explanation given earlier. For our optimized SEF conditions, we estimate a fluorophore distance of d = 1–1.5 nm and we measured an average SEF EF of 17× for R6G (whose Q_0 is 0.17), which would therefore correspond to 3× enhancement for Q_0 = 1. This is compatible with the predictions of Fig. 3(d) for the off-resonant case, although as emphasized earlier, comparison of absolute EF with theory is difficult because of the polydispersity of the aggregates. However, this optimized EF can also be compared with the one measured in non-optimized aggregated nanoparticles (≈2× for R6G, equivalent to 0.34× for Q_0 = 1). The relative enhancement by a factor of 10× is in qualitative agreement with the theoretical predictions of Fig. 2 for the average EF when the distance is changed from d = 0.2 nm to d = 1–1.5 nm.

Conclusions

In conclusion, we have shown that fluorescence enhancement in Dye-labeled DNA/Ag nanoparticles co-aggregates is on-par with the enhancement reported for nano-structured surfaces, while being much simpler to obtain than from top down approaches such as e-beam nanolithography. These results moreover highlight the possibility of efficient SEF from fluorophores located very close to metallic surfaces (d = 1–2 nm). We expect that this method of nanoparticle aggregation for enhancement of fluorescence can have interesting applications in the field of bioanalysis, where fluorescence is a common detection method. For detection of DNA, magnetic particle-based,[47] and microfluidic-based[48] systems have been developed with SERS-based readout using nanoparticle aggregates, and these could be easily adapted for SEF. In addition, higher enhancements are theoretically possible if the aggregation can occur specifically onto the labeled molecule, rather than have the molecules distributed uniformly over the nanoparticles surface. We are currently looking into such "targeted" approaches.[49]

Acknowledgements

The work of R. G. was supported by the European Commission (EC) through the Human Potential Programme within the 6th framework programme (Marie Curie ToK-DEV fellowship, MTKD-CT-2006-042410 LISA). ECLR is indebted to the Royal Society of New Zealand for support through a Marsden Grant and Rutherford Discovery Fellowship. We thank P. J. van der Zaag for comments on the manuscript.

Notes and references

1 S. Eustis and M. A. El-Sayed, *Chem. Soc. Rev.*, 2006, **35**, 209–217.
2 E. C. Le Ru and P. G. Etchegoin, *Principles of Surface-Enhanced Raman Spectroscopy*, Elsevier, Amsterdam, 2008.
3 R. Aroca, *Surface enhanced vibrational spectroscopy*, Wiley, Hoboken, NJ, 2006.
4 H. Metiu, *Prog. Surf. Sci.*, 1984, **17**, 153–320.
5 M. Moskovits, *Rev. Mod. Phys.*, 1985, **57**, 783–826.
6 E. C. Le Ru, C. Galloway and P. G. Etchegoin, *Phys. Chem. Chem. Phys.*, 2006, **8**, 3083–3087.
7 H. X. Xu, J. Aizpurua, M. Kall and P. Apell, *Phys. Rev. E: Stat. Phys., Plasmas, Fluids, Relat. Interdiscip. Top.*, 2000, **62**, 4318–4324.
8 E. C. Le Ru, E. Blackie, M. Meyer and P. G. Etchegoin, *J. Phys. Chem. C*, 2007, **111**, 13794–13803.
9 A. M. Glass, P. F. Liao, J. G. Bergman and D. H. Olson, *Opt. Lett.*, 1980, **5**, 368–370.
10 J. Gersten and A. Nitzan, *J. Chem. Phys.*, 1981, **75**, 1139–1152.
11 J. R. Lakowicz, Y. Shen, S. D'Auria, J. Malicka, J. Fang, Z. Gryczynski and I. Gryczynski, *Anal. Biochem.*, 2002, **301**, 261–277.
12 H. Szmacinski, J. R. Lakowicz, J. M. Catchmark, K. Eid, J. P. Anderson and L. Middendorf, *Appl. Spectrosc.*, 2008, **62**, 733–738.
13 P. P. Pompa, L. Martiradonna, A. Della Torre, F. Della Sala, L. Manna, M. De Vittorio, F. Calabi, R. Cingolani and R. Rinaldi, *Nat. Nanotechnol.*, 2006, **1**, 126–130.
14 Y. Chen, K. Munechika and D. S. Ginger, *Nano Lett.*, 2007, **7**, 690–696.
15 O. G. Tovmachenko, C. Graf, D. J. van den Heuvel, A. van Blaaderen and H. C. Gerritsen, *Adv. Mater.*, 2006, **18**, 91–95.
16 J. Zhang, Y. Fu, M. H. Chowdhury and J. R. Lakowicz, *J. Phys. Chem. C*, 2008, **112**, 9172–9180.
17 O. Stranik, R. Nooney, C. McDonagh and B. MacCraith, *Plasmonics*, 2006, **2**, 15–22.
18 F. Tam, G. P. Goodrich, B. R. Johnson and N. J. Halas, *Nano Lett.*, 2007, **7**, 496–501.
19 J. Zhang, Y. Fu, M. H. Chowdhury and J. R. Lakowicz, *Nano Lett.*, 2007, **7**, 2101–2107.
20 M. Ringler, A. Schwemer, M. Wunderlich, A. Nichtl, K. Kurzinger, T. A. Klar and J. Feldmann, *Phys. Rev. Lett.*, 2008, **100**, 203002.
21 J. Zhang, J. Malicka, I. Gryczynski and J. R. Lakowicz, *Anal. Biochem.*, 2004, **330**, 81–86.
22 C. M. Galloway, P. G. Etchegoin and E. C. Le Ru, *Phys. Rev. Lett.*, 2009, **103**, 063003.
23 J. Zhang, E. Matveeva, I. Gryczynski, Z. Leonenko and J. R. Lakowicz, *J. Phys. Chem. B*, 2005, **109**, 7969–7975.
24 D. M. Cheng and Q. H. Xu, *Chem. Commun.*, 2007, 248–250.
25 K. Aslan, I. Gryczynski, J. Malicka, E. Matveeva, J. R. Lakowicz and C. D. Geddes, *Curr. Opin. Biotechnol.*, 2005, **16**, 55–62.
26 P. Anger, P. Bharadwaj and L. Novotny, *Phys. Rev. Lett.*, 2006, **96**, 113002.
27 E. C. Le Ru, P. G. Etchegoin, J. Grand, N. Felidj, J. Aubard and G. Levi, *J. Phys. Chem. C*, 2007, **111**, 16076–16079.
28 V. V. Klimov and D. V. Guzatov, *Quantum Electron.*, 2007, **37**, 209–230.
29 P. G. Etchegoin, C. Galloway and E. C. Le Ru, *Phys. Chem. Chem. Phys.*, 2006, **8**, 2624–2628.
30 E. C. Le Ru, P. G. Etchegoin and M. Meyer, *J. Chem. Phys.*, 2006, **125**, 204701.
31 L. Novotny and B. Hecht, *Principles of Nano-Optics*, Cambridge University Press, 2006.
32 S. V. Gaponenko, *Introduction to Nanophotonics*, Cambridge University Press, 2010.
33 H. Chew, *J. Chem. Phys.*, 1987, **87**, 1355–1360.
34 P. Johansson, H. X. Xu and M. Kall, *Phys. Rev. B: Condens. Matter Mater. Phys.*, 2005, **72**, 035427.
35 E. C. Le Ru and P. G. Etchegoin, *Chem. Phys. Lett.*, 2006, **423**, 63–66.
36 P. C. Lee and D. Meisel, *J. Phys. Chem.*, 1982, **86**, 3391–3395.
37 N. Leopold and B. Lendl, *J. Phys. Chem. B*, 2003, **107**, 5723–5727.
38 S. M. Heard, F. Grieser, C. G. Barraclough and J. V. Sanders, *J. Colloid Interface Sci.*, 1983, **93**, 545–555.
39 D. Graham, W. E. Smith, A. M. T. Linacre, C. H. Munro, N. D. Watson and P. C. White, *Anal. Chem.*, 1997, **69**, 4703–4707.
40 J. Malicka, I. Gryczynski and J. R. Lakowicz, *Biochem. Biophys. Res. Commun.*, 2003, **306**, 213–218.
41 E. G. Matveeva, I. Gryczynski, A. Barnett, Z. Leonenko, J. R. Lakowicz and Z. Gryczynski, *Anal. Biochem.*, 2007, **363**, 239–245.

42 T. Liebermann and W. Knoll, *Colloids Surf., A*, 2000, **171**, 115–130.
43 K. Sokolov, G. Chumanov and T. M. Cotton, *Anal. Chem.*, 1998, **70**, 3898–3905.
44 P. J. Tarcha, J. DeSaja-Gonzalez, S. Rodriguez-Llorente and R. Aroca, *Appl. Spectrosc.*, 1999, **53**, 43–48.
45 A. Barnett, E. G. Matveeva, I. Gryczynski, Z. Gryczynski and E. M. Goldys, *Phys. B*, 2007, **394**, 297–300.
46 A. Kinkhabwala, Z. F. Yu, S. H. Fan, Y. Avlasevich, K. Mullen and W. E. Moerner, *Nat. Photonics*, 2009, **3**, 654–657.
47 D. Graham, B. J. Mallinder, D. Whitcombe, N. D. Watson and W. E. Smith, *Anal. Chem.*, 2002, **74**, 1069–1074.
48 F. T. Docherty, P. B. Monaghan, R. Keir, D. Graham, W. E. Smith and J. M. Cooper, *Chem. Commun.*, 2004, 118–119.
49 R. Gill and G. W. Lucassen, *Anal. Methods*, 2010, **2**, 445–447.

Electronic Supplementary Material (ESI) for Physical Chemistry Chemical Physics

Supporting Information for "Fluorescence enhancement at hot-spots: The case of Ag nanoparticle aggregates"

$M_{Loc,}$ M_{Tot} and M_{sef} as a function of position in a nanoparticle aggregate on and off resonance

The distributions of M_{Loc} and M_{Tot} on the surface are shown for two wavelengths (at resonance and off-resonance) in Fig S1(a) and S1(c) respectively. Note that, for simplicity, only calculations for dipolar emitters perpendicular to the surface are presented. The conclusions are the same for parallel dipoles. The fluorescence EFs, M_{SEF}, can then be deduced using Eq. 2, and their spatial distributions on the surface are shown in Fig. S1(b) and S1(d) (which are the same as Fig. 2(a-b) of the manuscript, repeated here for convenience), along with the average fluorescence EF $< M_{SEF} >$ for each case (this is the surface average for a random distribution of molecules on the dimer). Note that these average EF cannot be directly compared to experimental values, which are strongly influenced by the polydispersity of the colloidal aggregates, i.e. distribution of size, shape, orientation, and cluster size; all influencing the relative contribution of resonant vs non-resonant clusters. However, the predicted relative average SEF EF as the distance d of the fluorophores from the surface is changed can be meaningfully compared to the experimental results (note that for a distance of d=0.2nm, the local EM theory in principle no longer applies, but it was shown in Ref. 1 that such a small distance provides EM predictions in agreement with experiment. If non-local effects were included, a larger – and more realistic – distance would then give similar results).

Fig. S1 elucidates several of the properties of a nanoparticle dimer system, and by extrapolation of more complex aggregates. On the one hand, the total decay rate and therefore modified

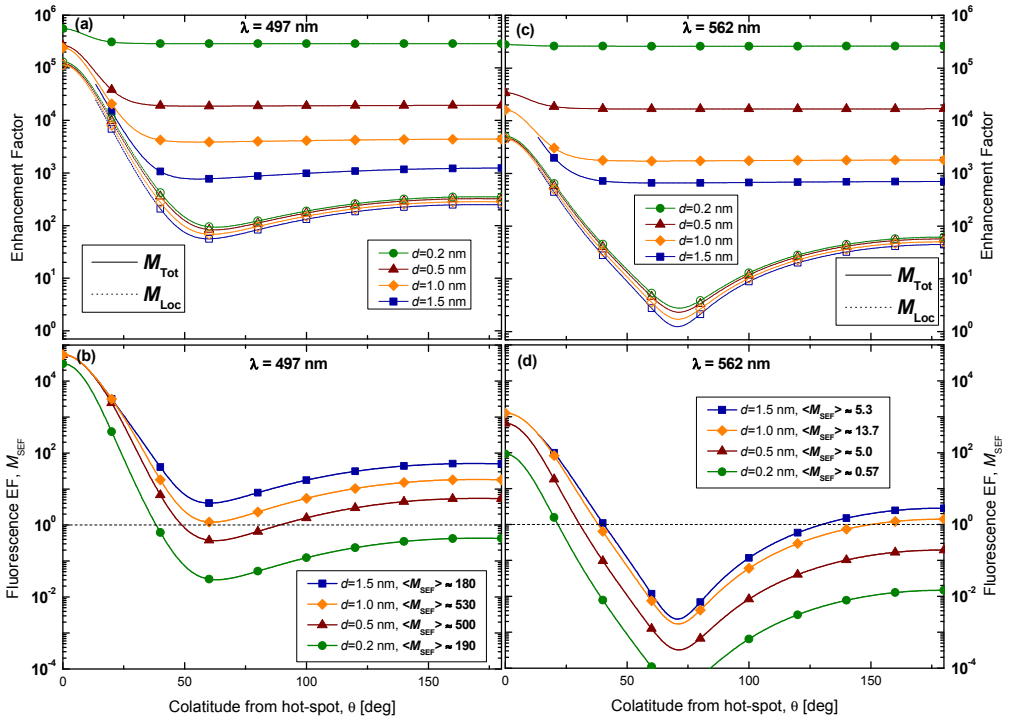

Fig. S1: Distribution of enhancement factors, M_{Loc}, M_{Tot}, and M_{SEF} (for the same dimer model as in Fig. 1) as a function of fluorophore position on the dimer surface, characterized by the colatitute (angle θ) from the hot-spot (i.e. θ = 0 in the gap). Note that the longitude (ϕ) dependence is negligible. (a) and (b), left-hand side, correspond to the optimal case, where excitation is resonant, while (c) and (d), right, represent the more common case of non-optimal conditions. Four distances, *d*, from the surface are considered. In the case of *d* = 1.5 nm, the distribution is cut-off below θ = 13 degrees because the fluorophores cannot fit in the gap while maintaining the same distance from the surface. The surface-averaged fluorescence EFs corresponding to these distributions are also given in (b) and (d).

quantum yield is extremely sensitive to distance from the surface (see Fig. S1 top), while the local field enhancement (relevant for absorption) hardly changes, at least at short distances. On the other hand, the total decay rate is independent of position (in fact it is dominated by non-radiative quenching into the metal), except at the hot-spot where its radiative component becomes important. As a result, contrary to what is generally assumed, very large fluorescence EF (up to 10^4) are predicted to occur at the hot-spot, even at ultra-short distances2. Also, fluorescence quenching is predicted everywhere outside the hot-spot at short distances (d=0.2nm). However, a distance of d=1nm is sufficient to increase the fluorescence signal of these molecules by several orders of magnitude. Moreover, the area around the hot spot that contributes to the fluorescence enhancement is increased as the distance from the surface is

increasing (going from d=0.2 to d=0.5nm and then to d=1nm). However, when this distance increases beyond half the dimer gap width, the fluorophores are no longer able to fit into the hot-spot. This causes the average enhancement to decrease as the distance from the surface increases. However, this "parking problem" is partially compensated by the beneficial effect of increasing d, and therefore even in this case, the average SEF EF decreases with distance much slower than the average SERS EF (see supporting information).

For resonant conditions (Fig. S1(a-b)), the radiative rate enhancement is so large in the hot-spot, that it dominates the total decay rate for most distances, giving very little difference between d=0.2nm and d=1nm. However, for non-optimal less-resonant conditions (Fig. S1(c-d)), the radiative rate is not enhanced as much and the total decay rate is dominated by non-radiative emission, making the effect of the distance from the surface much stronger. In polydisperse aggregates, we expect the latter situation to be relevant. Thus, we can predict, that even though for dye adsorbed to the surface, who will behave more closely to the case of d=0.2nm in Fig 2d, quenching might be observed, under similar conditions enhancement could be observed if the distance of the dye from the surface can be increased to 1-1.5nm. In the following, we therefore focus on providing an experimental demonstration of this effect in silver colloids aggregates, using dye-labelled DNA as a means to control the distance between fluorophore and surface.

Calculation of the average SERS EF of R6G

A reference standard – 0.88 nM R6G dye in ethanol, gave a reading of 2.3×10^{7} counts at 560 nm after spectral calibration correction (see Figure. S2). From the shape of R6G emission curve taken from PhotochemCAD 2[3], one can calculate the ratio of the integral area to the height of the signal at 560 nm to be 66 nm. Multiplying all these numbers gives 1.7×10^{9} counts×nm/nM for the total area of the fluorescence peak. For the strongest Raman peak at 1356 cm^{-1}, using 500 pM of R6G-labeled DNA and the aggregation that induces maximum SERRS signal, one can measure a total area of 2.0×10^{7} counts×nm/nM. This shows that the measured Raman signal of this peak is approx. 85x smaller than the fluorescence cross section of R6G. As the total fluorescence cross section of R6G is 4.36×10^{-16} cm^{2}, the integrated Raman peak cross section can be approximated as 5.13×10^{-18} cm^{2}. Comparing this to the latest estimation of the cross section of this peak using stimulated Raman emission technique[4] (2.6×10^{-23} cm^{2}), we can estimate the average SERRS enhancement in this system to be 2×10^{5}.

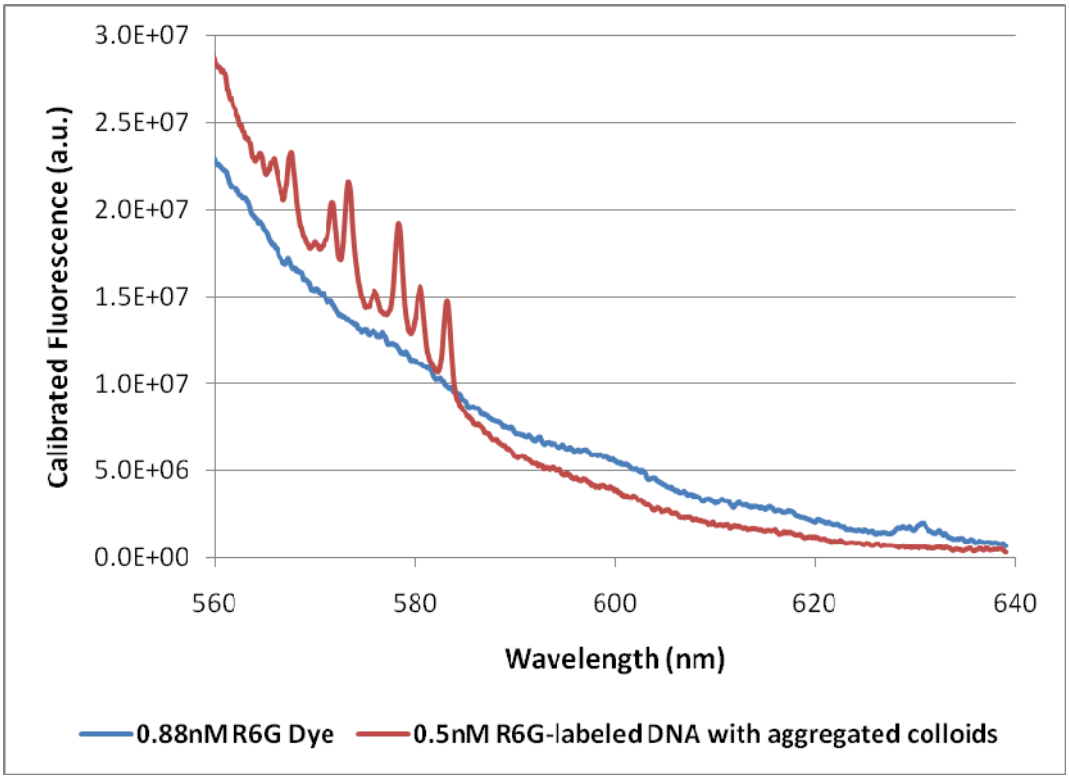

Figure S2: SERRS spectra of 500 pM R6G-labeled DNA with aggregated colloids, and Fluorescence spectra of 0.88 nM R6G dye in ethanol measured on the Raman spectrometer.

Overlap of dye spectra with the plasmon resonance peak of the Ag NPs aggregates

Figure S3(a) show the absorbance of non aggregated Ag NPs (red line) and aggregated Ag NPs (blue line). The spectrum of the aggregated particles were measured 20 sec after aggregation, which is the same time used in all SEF measurements. The aggregates absorbance peak is centered at about 530nm. The peak is wide because of the polydispersity in aggregate size and shape. Figure S3(b) shows the overlap between the absorbance spectra of the different dyes used and the wide absorbance peak of the Ag NP aggregates. The black line represent the wavelength of the laser excitataion (532 nm).

Table S1 gives the absorbance and emission peak data for the different dyes used. As can be seen all absorbance and emission frequencies are located under the central part of the plasmon peak of the aggregates.

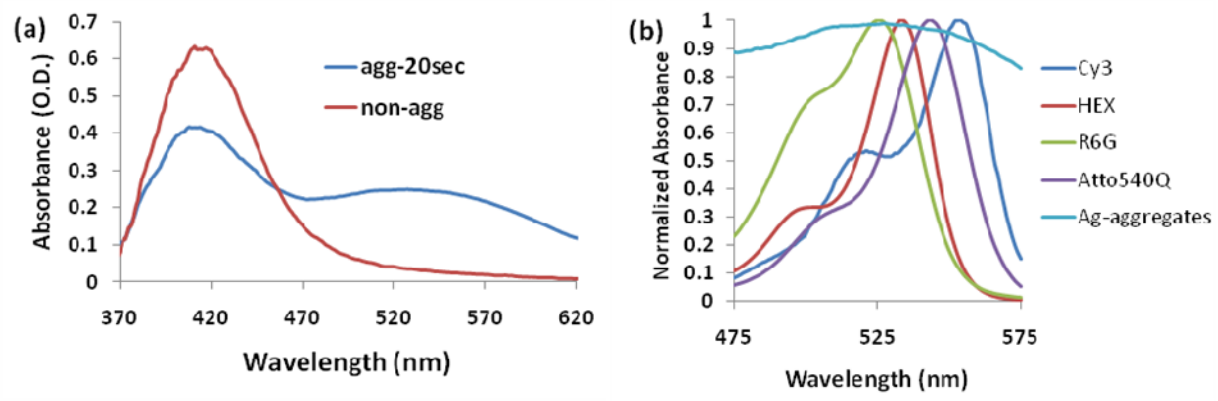

Figure S3 (a) Absorbance spectra of non aggregated (red line) and aggregated (blue line) Ag NPs. (b) Normalized absorbance spectra of the different dyes used in this study and the plasmon peak of the nanoparticle aggregates (from the measurement appearing in part (a) of this figure).

Dye	Max Abs (nm)	Max Ems (nm)
R6G	525	547
HEX	533	559
Atto 540Q	543	562
Cy3	554	566

Table S1: Absorbance and emission peak wavelength for the dyes used in this study.

Calculation of the quantum yield of dyes attached to DNA

The calculation of quantum yield for different dyes was done in a similar fashion to the calculation of the effective Raman cross section described in the previous paragraph. For any dye-labeled DNA, the total fluorescence signal at a known concentration was calculated by multiplying a measured point on the emission spectra (usually the maximal point) with the ratio of area to point height from the full fluorescence curve of the dye. This total calculated area was compared with the area of R6G dye in ethanol which has a known quantum yield of 95%. This ratio was further corrected for the ratio of extinction coefficients at 532 nm of the dye labeled DNA and R6G in ethanol.

Surface coverage of the DNA and effect of DNA concentration

In normal experiment, final concentration of DNA and Ag NPs were 500pM and 100pM respectively, giving a ratio of 5 DNA strands (29 bp, about 9.5nm fully stretched) for each 34nm diagmeter Ag NP. Even at the low salt concentration used, where the Debye length can reach 4nm, this would still give less than 20% of a full monolayer coverage. However, because spermine will bind the DNA and the nanoparticles, its effective concentration near the particles will be high, giving a much shorter Debye length than the one predicted above, and thus the DNA will amount to an even smaller percent of monolayer coverage. Figure S4 shows the fluorescence emission from experiments where 500pM of Cy3-DNA and 50pM of Cy3-DNA were used. The enhancement factor observed are x37 for the 500pM concentration and x39 for the 50pM concentration, which is only about 5% difference.

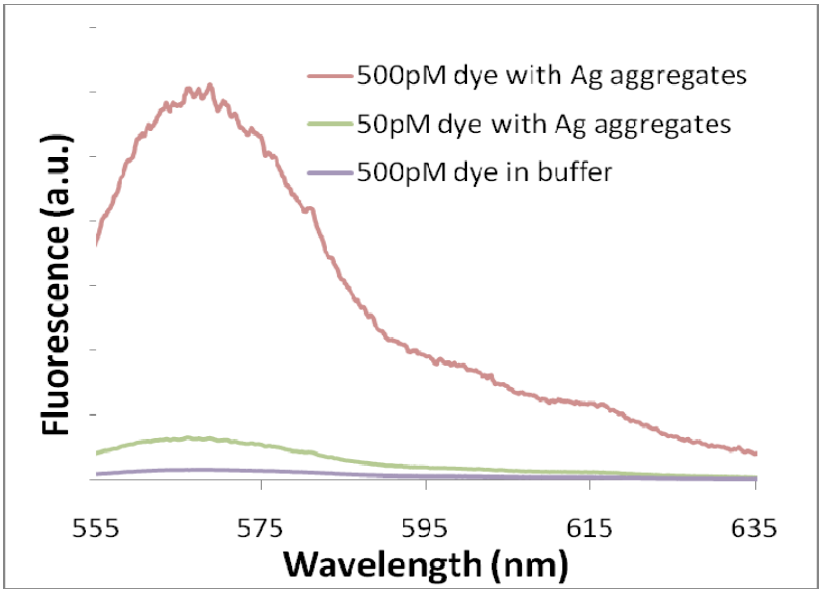

Figure S4 Fluorescence spectra of 500 pM dye-labeled DNA, in the presence (red line) and absence (purple line) of EDTA-coated silver nanoparticles (Ag-NPs), and 50pM dye-labeled DNA in the presence of Ag-NPs (green line). All experiments were conducted in a solution containing 20 µM Spermine, and 4 mM phosphate buffer pH=7.1. The NPs concentration when they were present was 100 pM. The DNA used was Cy3-DNA2.

Fluorescence enhancement of HEX-DNA2 and R6G-DNA2

The spectra used to estimate the average SEF EF of HEX-DNA2 and R6G-DNA2 are shown in Figure. S5.

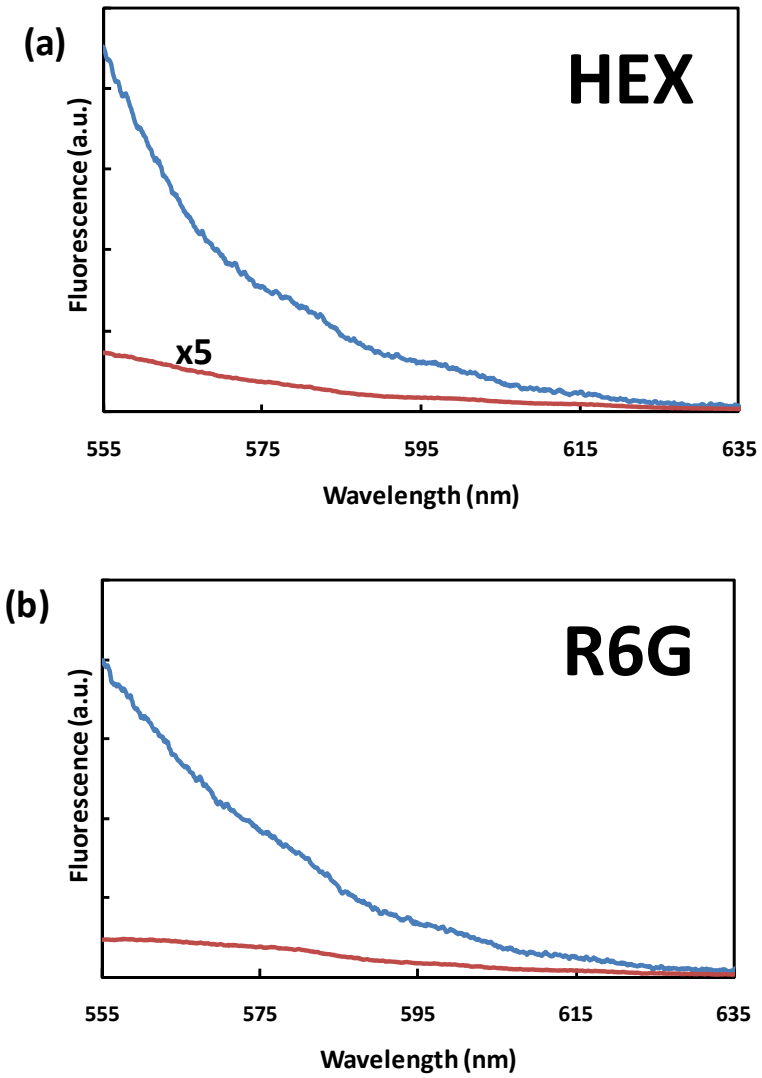

Figure S5 Fluorescence spectra of 500 pM dye-labeled DNA, in the presence (blue line) and absence (red line) of EDTA-coated silver nanoparticles (Ag-NPs). (a) HEX-conjugated to DNA-2, (b) R6G-conjugated to DNA-2. All experiments were conducted in a solution containing 20 μM Spermine, and 4 mM phosphate buffer pH=7.1. The NPs concentration when they were present was 100 pM.

Control experiments:

In order to show that only aggregated nanoparticles in the presence of dye-labeled DNA induce the enhanced fluorescence, several control experiments were performed, where one or more of the components (dye-labeled DNA, Spermine, Ag nanoparticles) were not added, but water/buffer was added instead. A typical set of measurements can be seen in Figure S6(a). Only for the HEX labeled DNA we observed a slight increase in fluorescence (x1.4) upon the addition of Ag nanoparticles (see figure S6(b)). In all other dye-DNA combinations, the dilution of dye-DNA in water gave the highest fluorescence.

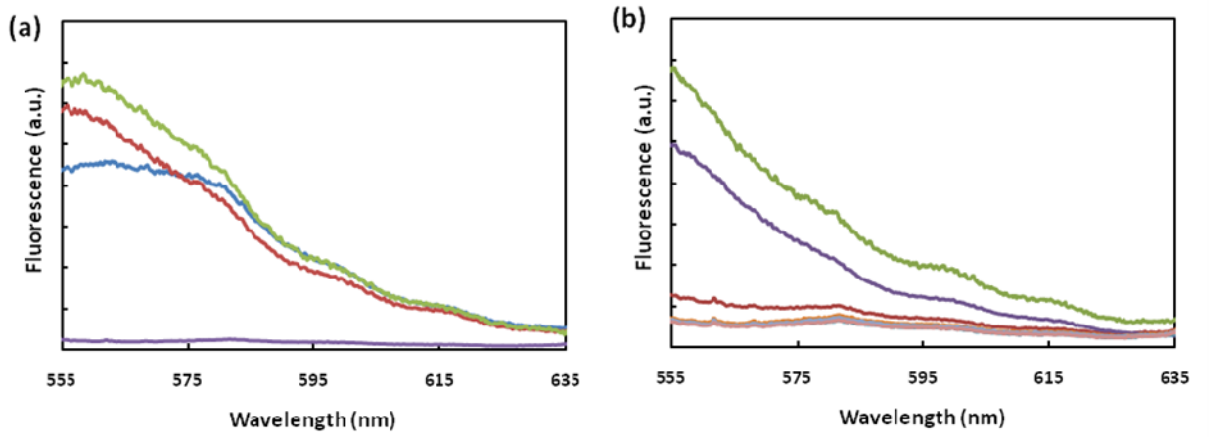

Figure S6: Fluorescence spectra of (a) 500 pM R6G-labeled DNA diluted in water (green line), 500pM R6G-labeled DNA in a solution containing 20 μM Spermine, and 4 mM phosphate buffer pH=7.1 without Ag-NPs (red line), 500pM R6G-labeled DNA in a solution containing 100pM Ag-NPs in 4mM phosphate buffer pH=7.1, but without Spermine (blue line), The background signal of a cuvette filled with triple-distilled water (violet line). (b) 500 pM HEX-labeled DNA diluted in water (violet line), 500pM HEX-labeled DNA in a solution containing 20 μM Spermine, and 4 mM phosphate buffer pH=7.1 without Ag-NPs (red line), 500pM HEX-labeled DNA in a solution containing 100pM Ag-NPs in 4mM phosphate buffer pH=7.1, but without Spermine (green line). The bottom line containes four overlapping graphs(from top to bottom): A solution containing 20 μM of Spermine, A solution containing 100pM of Ag-NPs, a solution containing both 20 μM of spermine and 100pM of Ag-NPs, triple distilled water. All the last four solutions were based on 4mM phosphate buffer and did not contain any dye-labeled DNA.

TEM microscopy:

Figure S7 shows a representative results from the TEM imaging of the nanoparticle aggregates. Both low and high resolution images are given for the same aggregates to show the nanoparticle size (apr. 34 ± 9 nm) and the interparticle distance (apr. 1-2 nm). As the aggregate is three dimentional, distances between particles can only be seen on the edges and not in the center of the aggregate.

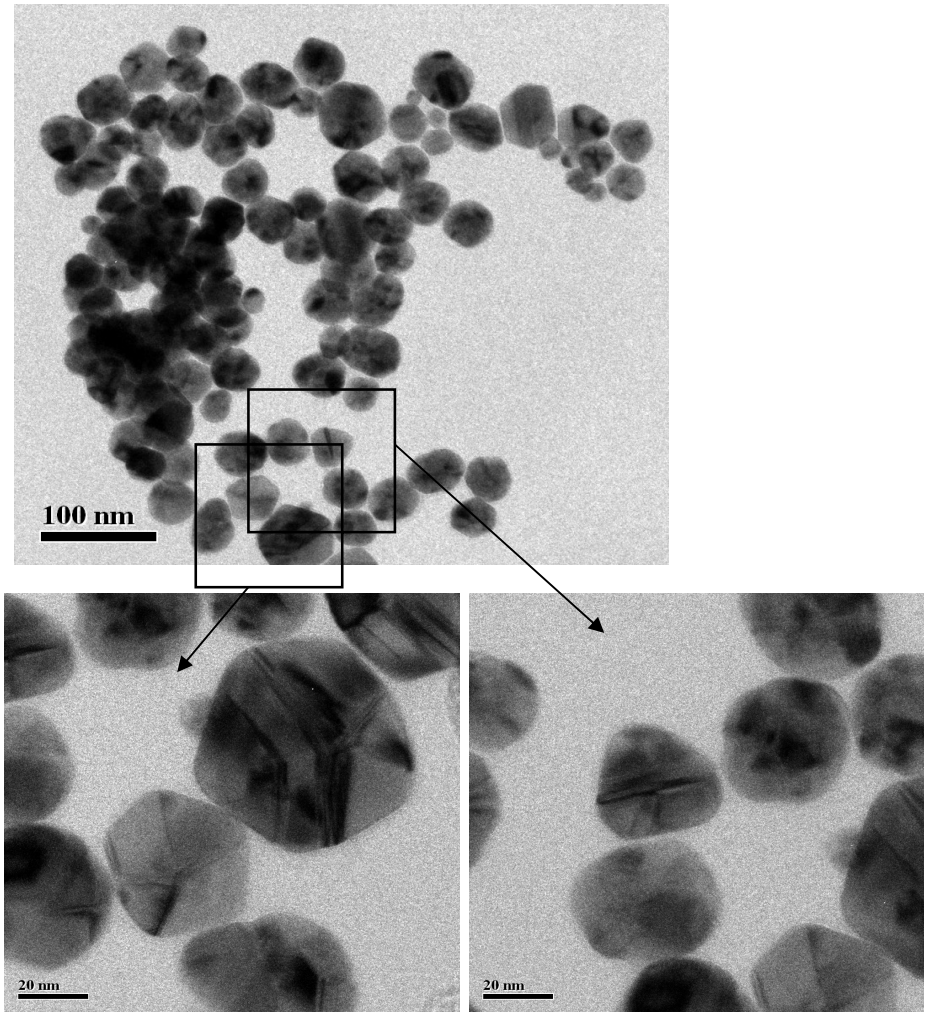

Figure S7: Transmission electron microscopy images of a nanoparticle aggregate. The top images was at x35000 and the bottom images were at x200000. Sample included 500pM R6G-labled DNA, 20 µM Spermine, and 100pM Ag-NPs in 4 mM phosphate buffer pH=7.1.

Theoretical calculations of the average SERS enhancement factor

Figure S7 shows the predicted distribution of SERS EF for molecules on the dimer at distances of d = 0.2, 0.5, 1, 1.5, and 2 nm from the metal surface. The geometrical parameters have been chosen as in the main text as the best estimates for our experiments: Ag sphere radius is 17 nm, gap between spheres is 2nm, embedding medium is water. The excitation wavelength is then chosen as the resonant wavelength for the particular structure here (497 nm), and the incident polarization is along the dimer axis. Similar results are obtained at 532 nm or 562 nm excitation or with other incident polarizations, only with smaller SERS EFs (see for example Table S1). Note that we are only interested in relative changes in the SERS EF distribution. The absolute value of the predicted SERS EF is irrelevant here, since predicting it would require averaging over the polydispersity of the aggregates and over their orientation[5].

Fig. S8 and Table S2 highlight several important aspects of the SERS EF distribution and average at a hot spot:

- The average SERS signal is dominated by molecules in a very small area around the hot-spot, typically less than 1% of the total area[5].
- The SERS intensities are not very sensitive to the distance from the surface at short distances (as opposed to the case of SEF, see main text).
- -However, as the molecules move away from the surface (and we assume that they must also remain the same distance away from the second sphere surface), they can no longer fit into the gap between the two colloids where the SERS EF is highest. This “parking problem” has a much more dramatic impact on the average SERS EF as the simple distance dependence of the SERS EF. For example, although the SERS EF at a given point

drops by a factor of only approx 1.4 when going from d = 1 nm to d = 1.5 nm, the average SERS EF drops by a factor of more than 10, simply because the points of highest enhancements at the hot-spot are no longer accessible to the molecule. It drops by another factor of 10 when going to d = 2 nm.

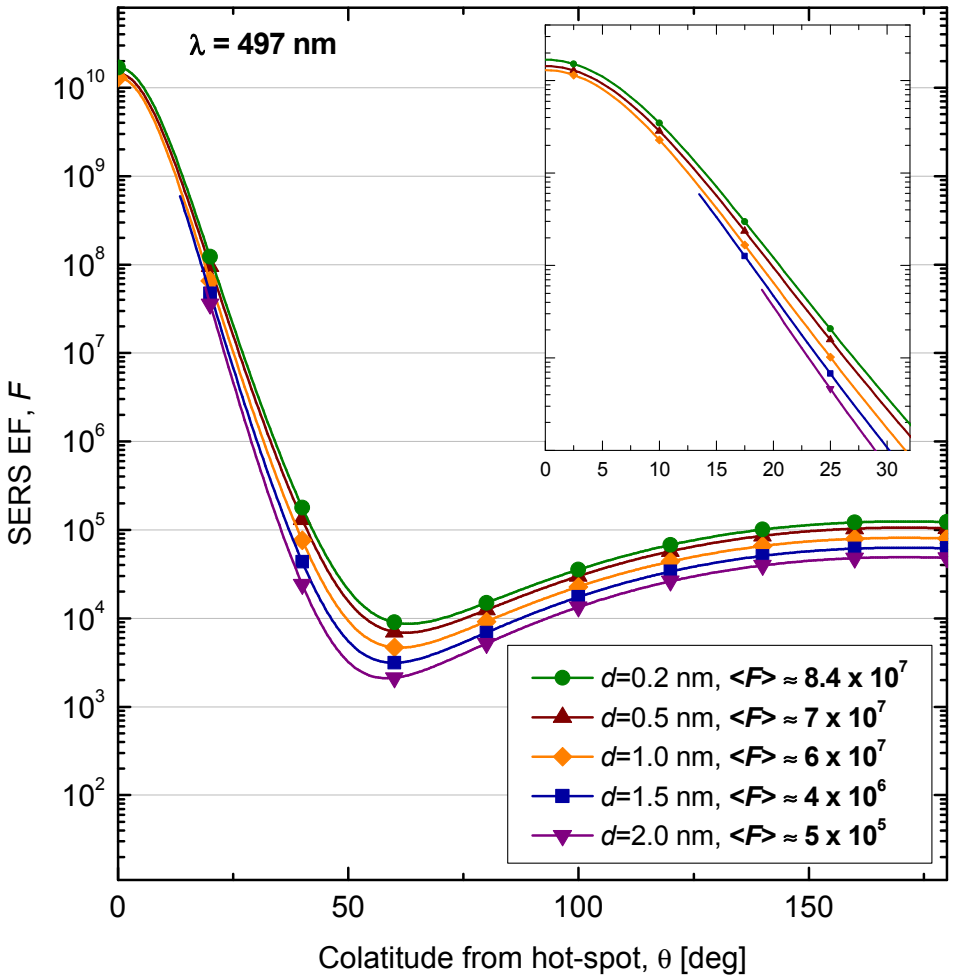

Figure S8: SERS enhancement factor, *F*, as a function of angle and distance from the surface of a silver dimer (34 nm diameter particles, 2 nm interparticle distance, embedded in water). For $d > 1$ nm, the distributions are cut-off at the point where the molecule can no longer fit in the gap while maintaining the same distance from the surface ("parking problem"). The corresponding average SERS EF are indicated in the legend. Although the punctual SERS EFs do not decrease substantially with *d*, the average SERS EFs drop sharply for $d > 1$ nm as a result of the parking problem. The inset shows a zoom of the region around the hot-spot.

Table S2: Summary of predicted surface-averaged SERS EF, $\langle F \rangle$ (calculated using Eq. 1 of the main text) for the same dimer structure as studied in Figure. S3, at three different excitation wavelengths.

Excitation wavelength	497 nm	532 nm	562 nm
d=0.2nm	8.4×10^7	1.5×10^6	1.6×10^5
d=0.5nm	7×10^7	1.3×10^6	1.3×10^5
d=1.0nm	3×10^7	1.1×10^6	1.1×10^5
d=1.5nm	4×10^6	1.0×10^5	1.3×10^4

Reproducibility of the fluorescence measurement in the presence of silver nanoparticle aggregate

In fig 6 of the main text, we claim that the spread in the measurement of the fluorescence enhancement is lower than the relative size of the marker used in the graph. This might seem counter-intuitive given the random nature of the aggregation process we employ to drive the fluorescence enhancement. However, it can be understood based on the fact that the measurement device we employ (R3000) uses a detection volume of 100um diameter. Therefore in this volume there are thousands of aggregates, that while they are not all the same size, their statistical average is determined by the initial volumes/concentration of the nanoparticle and aggregating agent solution used. Therefore, as long as we repeated mixing the same volume and same concentrations, the results repeated themselves with a very small coefficient of varience (CV) – see figure S9, black curves. However, it should be noted that the aggregating is a dynamic process, and therefore for reproducibility, the time of the measurement after the mixing is also important. As can be seen in figure S9, red curve, when measuring after 10% longer time (compared to t=20s which gave the optimal results), the fluorescence was 3% less.

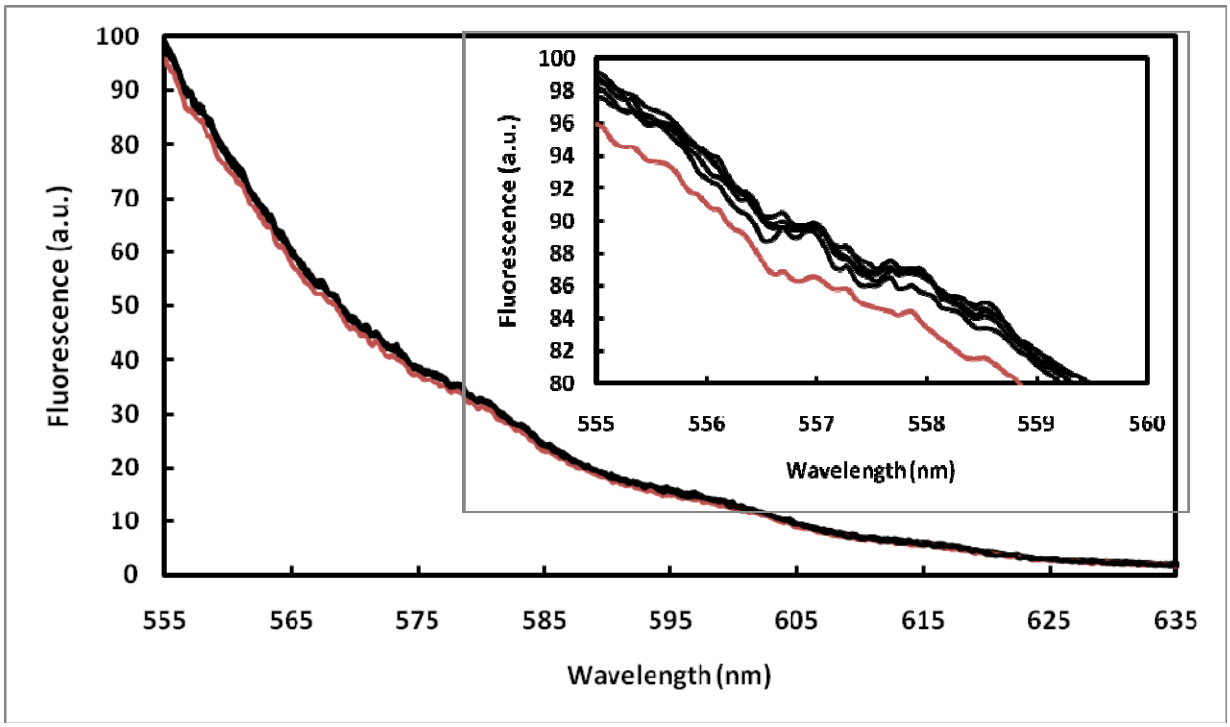

Figure S9: Fluorescence spectra of 500 pM R6G-DNA1 in the presence of EDTA-coated silver nanoparticles. The black curves are 5 repeates all measured 20s after mixing. The red curve is a 6th repeat mesured after 22s. In the insert appears a magnification of the same data from the top left corner of the main graph. All experiments were conducted in a solution containing 20 μM Spermine, and 4 mM phosphate buffer pH=7.1. The NPs concentration was 100 pM.

References:

1 C. M. Galloway, P. G. Etchegoin and E. C. Le Ru, *Phys. Rev. Lett.*, 2009, **103**, 063003.
2 E. C. Le Ru, P. G. Etchegoin, J. Grand, N. Felidj, J. Aubard and G. Levi, *J. Phys. Chem. C*, 2007, **111**, 16076-16079.
3 M. D. James, T. Masahiko and S. L. Jonathan, *Photochem. Photobiol.*, 2005, **81**, 212-213.
4 S. Sangdeok, M. S. Christina and A. M. Richard, *ChemPhysChem*, 2008, **9**, 697-699.
5 E. C. Le Ru, E. Blackie, M. Meyer and P. G. Etchegoin, *J. Phys. Chem. C*, 2007, **111**, 13794-13803.